HHS Public Access

Author manuscript

Biochim Biophys Acta Mol Basis Dis. Author manuscript; available in PMC 2020 July 01.

Published in final edited form as:

Biochim Biophys Acta Mol Basis Dis. 2019 July 01; 1865(7): 1865–1875. doi:10.1016/j.bbadis.2018.08.011.

Double Knockout of Akt2 and AMPK Predisposes Cardiac Aging without Affecting Lifespan: Role of Autophagy and Mitophagy

Shuyi Wang[1,2], **Machender R. Kandadi**[1], and **Jun Ren**[1,2]

[1]Center for Cardiovascular Research and Alternative Medicine, University of Wyoming, Laramie, WY 82071 USA

[2]Department of Cardiology and Shanghai Institute of Cardiovascular Diseases, Zhongshan Hospital, Fudan University, Shanghai 200032, China

Abstract

Increased age often leads to a gradual deterioration in cardiac geometry and contractile function although the precise mechanism remains elusive. Both Akt and AMPK play an essential role in the maintenance of cardiac homeostasis. This study examined the impact of ablation of Akt2 (the main cardiac isoform of Akt) and AMPKα2 on development of cardiac aging and the potential mechanisms involved with a focus on autophagy. Cardiac geometry, contractile, and intracellular Ca^{2+} properties were evaluated in young (4-month-old) and old (12-month-old) wild-type (WT) and Akt2-AMPK double knockout mice using echocardiography, IonOptix® edge-detection and fura-2 techniques. Levels of autophagy and mitophagy were evaluated using western blot. Our results revealed that increased age (12 months) did not elicit any notable effects on cardiac geometry, contractile function, morphology, ultrastructure, autophagy and mitophagy, although Akt2-AMPK double knockout predisposed aging-related unfavorable changes in geometry (heart weight, LVESD, LVEDD, cross-sectional area and interstitial fibrosis), TEM ultrastructure, and function (fractional shortening, peak shortening, maximal velocity of shortening/relengthening, time-to-90% relengthening, intracellular Ca^{2+} release and clearance rate). Double knockout of Akt2 and AMPK unmasked age-induced cardiac autophagy loss including decreased Atg5, Atg7, Beclin1, LC3BII-to-LC3BI ratio and increased p62. Double knockout of Akt2 and AMPK also unmasked age-related loss in mitophagy markers PTEN-induced putative kinase 1 (Pink1), Parkin, Bnip3, and FundC1, the mitochondrial biogenesis cofactor PGC-1α, and lysosomal biogenesis factor TFEB. In conclusion, our data indicate that Akt2-AMPK double ablation predisposes cardiac aging possibly related to compromised autophagy and mitophagy.

Correspondence to:Dr. Jun Ren, University of Wyoming College of Health Sciences, Laramie, WY 82071, USA, Tel: 307-766-6131; Fax: 307-766-2953; jren@uwyo.edu.

Author Contribution

SW, MRK: Designed the experiments, conducted the study; SW, JR: Drafted the manuscript.

6. **COMPETING INTERESTS:** The authors have declared that no competing interests exist.

Keywords

Akt2; AMPK; aging; autophagy; cardiac geometry; contractile function

1. INTRODUCTION

Increased age leads to a gradual deterioration of cardiac function and cardiac reserve as well as progressive cardiac remodeling manifested as cardiac hypertrophy and interstitial fibrosis [1–5]. To-date, a number of scenarios have been postulated for the pathogenesis of cardiac aging including inflammation, lipotoxicity, oxidative stress, apoptosis, mitochondrial injury, autophagy dysregulation and intracellular Ca^{2+} mishandling [6–9]. Nonetheless, the precise machineries behind progression of cardiac aging are still undefined. Recent findings from our lab and others have suggested a potential role for the essential survival signaling molecule protein kinase B (Akt) and the energy metabolism fuel AMP-dependent protein kinase (AMPK) in age- or aginginduced pathological changes in the heart [10–13]. The Akt signaling pathway, in particularly in response to insulin and insulin-like growth factor-1 (IGF-1), functions as an integrator rudimentary to growth and development, lifespan, healthspan and aging [10, 14]. AMPK, on the other hand, governs the energy metabolism with AMPK activation in response to resveratrol and metformin exhibiting anti-aging properties [12, 15]. Recent data from our group and others have suggested an essential role for autophagy, a highly conserved lysosomal process for degradation and recycling of proteins and organelles, in biological and cardiac aging [6, 16, 17]. Mammalian aging is associated with autophagy failure while autophagy induction prolongs lifespan and retards cardiac aging, in association with improved clearance of protein aggregate [18–20]. Given the essential role for Akt and AMPK in the regulation of cardiac survival and lifespan [21, 22], this study was designed to examine the role of ablation of Akt2 (the cardiac isoform of Akt) and AMPK on age-induced changes in geometry, function and intracellular Ca^{2+} homeostasis in the heart, with a special focus on autophagy and mitochondrial selective autophagy (mitophagy). Protein markers of autophagy and mitophagy including phosphatase and tensin homolog (PTEN)-induced kinase 1 (PINK 1), Parkin, Fun 14 domain containing 1 (FundC1) and BCL2/adenovirus E1B 19-kDa interacting protein 3 (BNIP3) were examined in young or old mouse hearts. We also evaluated the levels of the helix-loop-helix transcription factor EB (TFEB) as increased lifespan may be associated with activation of TFEB and lysosomal biogenesis [23].

2. METHODS AND MATERIALS

2.1: Generation of double knockout mice and Kaplan–Meier survival:

All animal procedures were approved by the Animal Care and Use Committees at the University of Wyoming (Laramie, WY, USA) and Zhongshan Hospital, Fudan University (Shanghai, China). Akt2 knockout mice were obtained from Dr. Morris Birnbaum at the University of Pennsylvania (Philadelphia, PA, USA) and AMPKα2 knockout mice were generated and characterized by Dr. Benoit Viollet at the Institut Cochin, Université Paris Descartes, CNRS (UMR 8104), Paris, France [24, 25]. $Akt2^{-/-}$ and $AMPK\alpha2^{-/-}$ mice (on C57BL/6 background) were cross-bred to generate the heterozygotes, which were further

crossed to generate Akt2$^{-/-}$-AMPKα2$^{-/-}$ (DKO) mice. To confirm genotypes, genomic DNA prepared from tail snips was analyzed using PCR. Mice were housed under temperature-controlled conditions (22 ± 2°C), humidity (55 ± 5%) and a 12 h/12 h light-dark circadian cycle with access to food and water *ad libitum*. All mice used for life span analysis (the Kaplan–Meier survival curve and the log rank test) were assigned to a longevity cohort at birth and were not used for any other tests.

2.2: Echocardiographic assessment:

Animals were anesthetized using ketamine (80 mg/kg, i.p.) and xylazine (12 mg/kg i.p.,) prior to the echocardiographic assessment. 2-D guided M-mode echocardiography were applied to examine mouse cardiac geometry and function using the Phillips Sonos 5500 machine (Phillips Medical Systems, Andover, MD, USA). The measurement processes were carried out following previous protocols [16].

2.3: Cardiomyocyte isolation, shortening/relengthening and intracellular Ca^{2+} handling:

Langendorff perfusion system were employed to isolate cardiomyocytes from wild type (WT) and Akt2$^{-/-}$-AMPKα2$^{-/-}$ (DKO) mice hearts following previous protocols [16]. Cardiomyocyte contractile function was monitored using a SoftEdge MyoCam® system (IonOptix Corporation, Milton, MA, USA) with an IX-70 Olympus inverted microscope [16]. Contractile buffer containing (in mM) NaCl 131, KCl 4, $CaCl_2$ 1, $MgCl_2$ 1, glucose 10 and HEPES 10 was added and cells were electrically challenged at 0.5 Hz. Contractile curve was recorded for each cell and the following indices were obtained: peak shortening (PS), maximal velocity of shortening (+ dL/dt), maximal velocity of relengthening (− dL/dt), time-to-PS (TPS), and time-to-90% relengthening (TR_{90}). The fura-2 dye Fura-2/AM (500 nM) was loaded on isolated cardiomyocytes for 10 min prior to fluorescence intensity recording. Fluorescence emissions were detected using a fluorescence photomultiplier tube (Ionoptix, Milton, MA). Alterations in fura-2 fluorescence intensity (FFI) were quantitated from the FFI ratio at 360 nm and 380 nm. Intracellular Ca^{2+} clearance was assessed by fluorescence decay time.

2.4: Evaluation of myocardial morphology:

After sedation, hearts were excised, rinsed briefly with PBS and immediately placed in a formalin solution for a day. The specimens were enclosed in paraffin, cut into thin (5 μm) sections and were labeled with fluorescein isothiocyanate (FITC) jointed wheat germ agglutinin. Images of cardiac section were taken using a digital microscope (×400). Cardiomyocyte cross-section area was calculated using the Image J (version1.34S) software [16]. Cardiac fibrosis formation was examined using the Masson's trichrome staining. Fibrosis (blue staining) can be differentiated from normal cardiac muscle tissue (red staining). The percentage of fibrosis was achieved by calculating the percentage of the light blue colored region among the entire area [16].

2.5: Electron microscopy:

The myocardial ultrastructure was evaluated using transmission electron microscopy. In brief, mouse heart from each experiment group was perfused and fixed with PIPES-buffered

formaldehyde-glutaraldehyde. Left ventricular myocardium was taken from the mid-ventricular region and was trimmed to 1 mm3 blocks. The blocks were fixed using a 10:1 fluid/tissue ratio overnight at 4 °C. After washing with PIPES buffer along with 2% sucrose (pH 7.4), myocardial blocks were further processed in PIPES buffered 1% OsO4 along with 2% sucrose and 1.5% K3FE(CN)6·3H2O overnight at 22–24 °C. The blocks were then dehydrated using graded ethanol and propylene oxide, and were ultimately enclosed in Epon/Araldite. RMCMTXL ultramicrotome and a Diatome diamond knife were used to obtain thin sections. Sections were labeled with lead citrate and uranyl acetate (in absolute ethanol). Micrographic pictures were taken using a Hitachi 7500 transmission electron microscope [16].

2.6: Western blot analysis:

Myocardial samples of 50 μg were separated in 10%–15% SDS-PAGE gels and were transferred onto nitrocellulose membranes. Following block, the membranes were incubated with the anti-Akt1, anti-Akt2, anti-Akt3, anti-AMPKα2, anti-p16, anti-p21, anti-Atg5, anti-Atg7, anti-Beclin1, anti-LC3B, anti-p62, anti-Parkin, anti-Bnip3, anti-PGC-1α, anti-TFEB (1:1000, Cell Signaling Technology, Danvers, MA, USA), anti-FundC1, anti-UCP2, anti-Pink1, (1:1000; Abcam, Cambridge, MA, USA), anti-GAPDH and anti-tubulin (loading controls) (1:1000; Cell Signaling Technology, Danvers, MA, USA) antibodies. After washing in Tris-buffered saline-Tween (TBST), nitrocellulose membranes were co-treated with horseradish peroxidase (HRP)-coupled secondary antibodies for 1 h at room temperature. A Bio-Rad Calibrated Densitometer was employed to scan the film and intensity of immunoblot bands was normalized to that of the loading control (GAPDH or α-tubulin) [16].

2.7: Data analyses:

Data were shown mean with standard error (Mean ± SEM). A p value < 0.05 was set for statistical significance using one-way analysis of variation (ANOVA). The Tukey's test was used for post hoc analysis. The log-rank test was performed for Kaplan-Meier survival curve.

3. RESULTS

3.1: General characteristics, biometrics and survival in WT and DKO mice

The biometric profiles of young or old WT and DKO mice are summarized in Table 1. Increased age prompted a slightly higher body weight (13.5% in WT mice and 19.6% in DKO mice, although not statistically significant). Increased age led to an increase in organ weight in both WT mice and DKO mice, yet not significant when normalized to whole body weight (liver, kidney, and spleen). Interestingly, DKO seemed to induce cardiac hypertrophy at the age of 12 months, compared to their WT counterpart, even after normalized to whole body weight (36.2% in heart weight, 14.2 % in heart-to-body weight). Although serum insulin and triglyceride levels were elevated in 12 month-old mice compared to 4 month-old counterparts in both WT and DKO groups, neither increased age nor Akt2-AMPK ablation, or both, overtly altered blood glucose levels (Table 1). Ablation of Akt2 and AMPKα2 was confirmed using Western blot analysis. Expression of Akt2 isoform and AMPKα2 subunit

was completely absent in DKO mice, without eliciting any effect on other Akt isoforms (Akt1 and Akt3) (Fig. 1A, F-H). Aging itself did not affect the levels of Akt isoforms and AMPKα2. DKO failed to alter the course of aging, as evidenced by a comparable increase in the levels of senescence markers p16 and p21 in 12-month-old mice, regardless of the genetic background (Fig. 1C-D). There was no observable difference in life span between WT and DKO mice, with a median survival of 33 and 36 months, respectively (Fig. 1B).

3.2: Myocardial geometry and contractile function

Neither increased age not Akt2-AMPKα2 ablation, or both, overtly affected heart rate or left ventricular wall thickness. Likewise, neither increased age not Akt2-AMPKα2 ablation affected heart weight, fractional shortening, LV end systolic and diastolic diameters (LV ESD and LV EDD) although the combination of the two prompted cardiac hypertrophy (normalized to body weight), cardiac remodeling (increased LV ESD and LV EDD) and impaired fractional shortening (Fig. 2).

3.3: Cardiomyocyte contractile function and intracellular Ca^{2+} transient properties

The 12 month-old WT mice exhibited the same contractile function as their younger counterparts. While the 4 month-old DKO mice exhibited comparable mechanical profiles as the WT groups, 12 month-old DKO mice showed decreased peak shortening, maximal velocities of shortening/ relengthening (± dL/dt), and prolonged time-to-90% relengthening (TR_{90}), sparing resting cell length and time-to-peak shortening (TPS) (Fig. 3A-F).

To explore possible mechanisms between increased age and Akt2-AMPKα2 double ablation, intracellular Ca^{2+} handling was evaluated using fura-2 fluorescence techniques. Our data revealed that neither increased age nor Akt2-AMPKα2 ablation significantly affected resting intracellular Ca^{2+} levels, yet the combination of the two significantly decreased the electrically-stimulated rise in intracellular Ca^{2+} (ΔFFI) and impaired intracellular Ca^{2+} clearance ability (Fig. 4 A-C). These data together suggested that Akt2-AMPKα2 ablation accelerated cardiomyocyte contractile dysfunction at an early age, compared with normal aging-induced cardiac dysfunction, which happened after 24 months [10, 16].

3.4: Myocardial histology and ultrastructure in 4- or 12 month-old WT and DKO mice

To assess the impact of increased age and Akt2-AMPKα2 ablation on cardiac remodeling in aging, myocardial histology including cardiomyocyte cross-section and interstitial fibrosis was examined. Lectin staining revealed an increased cardiomyocyte transverse cross-sectional area in 12 month-old DKO mice but not in other groups, consistent with increased LV mass and heart weights. Little effect was noted in cardiomyocyte cross-sectioning from 4 month-old DKO group (Fig. 5A and D). Masson's Trichrome staining revealed that 12 month-old DKO mice exhibited enhanced interstitial fibrosis, the effect of which was not observed in 12 month-old WT mice nor 4 month-old DKO mice (Fig. 5B and E). Ultrastructure of mitochondria and sarcomere in the hearts were studies using transmission electronic microscopy (TEM). The images revealed that sarcomeres and myocardial filaments were severely distorted, accompanied with mitochondrial swelling in the 12 month-old DKO mice, but not in other experimental groups (Fig. 5C). These data together

suggested that DKO caused cardiac hypertrophy and collagen deposition at an early age, causing premature aging of the heart.

3.5: Autophagy and mitophagy level in 4- or 12 month-old WT and DKO mice

To elucidate the mechanisms of action behind the acceleration of DKO-induced cardiac mechanical and intracellular Ca^{2+} responses, levels of autophagy and mitophagy were examined. Our data depicted that while 12 months of age was not able to trigger any significant changes in autophagy markers including Atg5, Atg7, Beclin-1, LC3B and p62, Akt2-AMPKα2 overtly downregulated these autophagy protein markers (Atg5, Atg7, Beclin-1 and LC3B) while elevating that of autophagosome adaptor protein p62 with aging. Akt2 and AMPKα2 ablation did not affect these autophagy protein markers at 4 months of age (Fig 6 A-H). Furthermore, our data revealed that in 12 month-old DKO mice, all 3 pathways of mitophagy were down-regulated, as evidenced by decreased levels of mitophagy protein markers PINK1-Parkin, BNIP3 and FundC1 (Fig 7A-E). Although increased age and Akt2-AMPKα2 did not affect the levels of mitochondrial proteins UCP2 and PGC-1α, or lysosomal transcription factor EB (TFEB), the combination of the two overtly downregulated the levels of UCP2, PGC-1α and TFEB (Fig. 7F-H), indicating impaired mitochondrial and lysosomal biogenesis.

4. DISCUSSION

The salient findings from our current study suggested that ablation of Akt2 and AMPK predisposed premature cardiac aging or age-induced changes in cardiac geometry, contractile and intracellular Ca^{2+} properties. The Akt2-AMPK ablation-induced changes in cardiac geometry and function were associated overt cardiac remodeling as manifested by cardiac hypertrophy and interstitial fibrosis. In addition, Akt2-AMPK double ablation unmasked age-associated loss in autophagy, mitophagy, mitochondrial integrity and lysosomal biogenesis. These results suggest a possible permissive role of Akt2-AMPK signaling in the predisposition of cardiac aging possible related to loss of autophagy and mitophagy in the heart.

Increased age is commonly associated with unfavorable cardiac remodeling and function including cardiac hypertrophy, interstitial fibrosis, compromised contractility and prolonged diastolic duration [26–28]. Here we did not observe any changes in cardiac geometry, remodeling (heart and cardiomyocyte size, interstitial fibrosis), intracellular Ca^{2+} regulation, and contractile function in 12-month-old mid-age murine hearts. Interestingly, Akt2-AMPK ablation unmasked age-induced unfavorable changes in cardiac geometry and function. Although double knockout of Akt2 and AMPK itself did not elicit any overt changes in cardiac geometry, function and intracellular Ca^{2+} handling, prominent changes in heart size, cardiomyocyte cross-sectional area, and interstitial fibrosis were noted in 12-month-old Akt2-AMPK knockout mice, favoring an important role for lost Akt2/AMPK signaling in the predisposition of cardiac aging. Akt2-AMPK knockout did not affect the Kaplan-Meier survival rate nor did it affect the senescence markers p16 and p21, indicating that Akt2-AMPK ablation did not overtly alter the course of biological aging. In addition, Akt2-AMPK double knockout failed to elicit notable cardiac geometric or morphological effects

at young age, suggesting that ablation of Akt2-AMPK takes time to impose notable cardiac remodeling and contractile effects. Cardiac remodeling (hypertrophy and interstitial fibrosis) are usually noted with increased age and contributes to transition from the physiological remodeling to pathological remodeling, en route to unfavorable changes in heart function [26]. Although Akt2-AMPK ablation failed to alter intracellular Ca^{2+} handling at the young age, it unmasked intracellular Ca^{2+} handling defects with increased age, which contributes to cardiac contractile dysfunction. Moreover, our data did not reveal any notable change in Akt1 and Akt3 isozymes with Akt2 ablation at both age points, thus excluding possible compensatory contribution from these Akt isozymes. It is noteworthy that deletion of Akt2 was reported to trigger onset and development of type 2 diabetes mellitus with time [25, 29] although our study did not note the presence of diabetic phenotype at both ages tested in our study.

The Akt2-AMPK knockout-induced predisposition of increased age-related changes in cardiac contractile function coincided with worsened mitochondrial integrity (UCP2, PGC-1α and ultrastructure), autophagy (Beclin-1, LC3B, Atg5, Atg7 and p62) and mitophagy (PINK1, Parkin, FUNDC1 and BNIP3) as well as lysosomal biogenesis (TFEB). These findings suggested a possible role of autophagy, in particular mitochondrial autophagy (mitophagy) in Akt2-AMPK ablation-induced changes in cardiac geometry and function. Autophagy is capable of preserving diastolic function in senescent myocardium through protection of intracellular Ca^{2+} homeostasis [30]. Several theories may contribute to the Akt2-AMPK ablation-elicited responses with aging. First, our earlier findings revealed compromised phosphorylation of the Akt negative regulator PTEN in association with Akt overactivation with aging [11]. More evidence suggested a finetone of Akt signaling in aging process, regardless of intact AMPK signaling. Chen and coworkers suggested that sodium hydrosulfide attenuates aging process via PI3K-Akt-mediated regulation of mitochondrial integrity and oxidative stress [31]. Second, loss of autophagy and mitophagy may contribute to Akt2-AMPK ablation-induced unfavorable geometric and functional response. Activation of Akt, an essential signaling molecule for cardiac survival and mitochondrial function [32, 33], has been shown to suppress autophagy, in a manner reminiscent of aging [11, 32, 34–38]. Paradoxically, our current results revealed that Akt2-AMPK ablation downregulated autophagy and mitophagy with increased age. Although our earlier study suggested that Akt2 knockout may restore autophagy and mitophagy with aging [39], such protective effect no longer prevails with AMPK deficiency. The various reported effects of Akt2 knockout on autophagy seem puzzling although the presence of AMPK appears to be vital. Numerous findings suggested the permissive role of AMPK in the preserved autophagy and resistance to aging process [31, 40]. Our earlier data supported a likely contributing role of AMPK deficiency in cardiac aging [12]. Third, our data support a role for mitophagy and mitochondrial integrity in Akt2-AMPK ablation-induced cardiac aging. In our hands, Akt2-AMPK knockout unmasked age-induced changes in mitochondrial biogenesis cofactor PGC-1α and mitochondrial ultrastructure with suppressed mitophagy protein markers. Our study also revealed a possible role of compromised lysosomal function as evidenced by decreased TFEB in Akt2-AMPK double knockout hearts. With aging, autophagy gradually declines, largely due to the decreased formation of autophagic vacuoles and compromised fusion of these vacuoles with lysosomes [41, 42].

Experimental limitations: Our current study suffers from a number of limitations. First and perhaps the foremost, our results failed to offer the precise interplay among mitophagy, cardiac geometry and function in cardiac aging process. Use of more unique animal models of autophagy or mitophagy will offer better understanding with regards to the role of autophagy or mitophagy in the progression of cardiac aging. Next, although our study revealed a role for TFEB in Akt2-AMPK double ablation-induced cardiac anomalies, little information is available on how TFEB-related lysosomal function contributes to the compromised autophagy/mitophagy.

In summary, our findings suggest that Akt2-AMPK double knockout plays an essential role in the predisposition of age-related unfavorable change in cardiac geometry and function. Our data favor the notion that failure in autophagy and mitophagy with Akt2-AMPK ablation may underscore the premature cardiac aging with ablation of these essential cardiac signaling molecules. Although our study sheds some light on the role of Akt-AMPK signaling cascades on autophagy and cardiac homeostasis, the onset and development of premature cardiac aging, particularly in association with mitophagy still require in depth exploration.

ACKNOWLEDGMENTS

This work was supported in part by grants from the National Institute of Health/National Institute of Aging (R03 AG21324), and the National Natural Science Foundation of China (91749128, 81521001).

References

[1]. Feridooni HA, Dibb KM, Howlett SE, How cardiomyocyte excitation, calcium release and contraction become altered with age, J Mol Cell Cardiol, 83 (2015) 62–72. [PubMed: 25498213]

[2]. Barton GP, de Lange WJ, Ralphe JC, Aiken J, Diffee G, Linking metabolic and contractile dysfunction in aged cardiac myocytes, Physiological reports, 5 (2017).

[3]. de Lucia C, Wallner M, Eaton DM, Zhao H, Houser SR, Koch WJ, Echocardiographic Strain Analysis for the Early Detection of Left Ventricular Systolic/Diastolic Dysfunction and Dyssynchrony in a Mouse Model of Physiological Aging, The journals of gerontology. Series A, Biological sciences and medical sciences, (2018).

[4]. Frimat M, Daroux M, Litke R, Neviere R, Tessier FJ, Boulanger E, Kidney, heart and brain: three organs targeted by ageing and glycation, Clinical science, 131 (2017) 1069–1092. [PubMed: 28515343]

[5]. Feridooni HA, Kane AE, Ayaz O, Boroumandi A, Polidovitch N, Tsushima RG, Rose RA, Howlett SE, The impact of age and frailty on ventricular structure and function in C57BL/6J mice, The Journal of physiology, 595 (2017) 3721–3742. [PubMed: 28502095]

[6]. Nakayama H, Nishida K, Otsu K, Macromolecular Degradation Systems and Cardiovascular Aging, Circulation research, 118 (2016) 1577–1592. [PubMed: 27174951]

[7]. Narasimhan M, Rajasekaran NS, Cardiac Aging - Benefits of Exercise, Nrf2 Activation and Antioxidant Signaling, Advances in experimental medicine and biology, 999 (2017) 231–255. [PubMed: 29022266]

[8]. Shi R, Guberman M, Kirshenbaum LA, Mitochondrial quality control: The role of mitophagy in aging, Trends in cardiovascular medicine, 28 (2018) 246–260. [PubMed: 29287956]

[9]. Zhang Y, Mi SL, Hu N, Doser TA, Sun A, Ge J, Ren J, Mitochondrial aldehyde dehydrogenase 2 accentuates aging-induced cardiac remodeling and contractile dysfunction: role of AMPK, Sirt1, and mitochondrial function, Free Radic Biol Med, 71 (2014) 208–220. [PubMed: 24675227]

[10]. Ren J, Yang L, Zhu L, Xu X, Ceylan AF, Guo W, Yang J, Zhang Y, Akt2 ablation prolongs life span and improves myocardial contractile function with adaptive cardiac remodeling: role of Sirt1-mediated autophagy regulation, Aging Cell, 16 (2017) 976–987. [PubMed: 28681509]

[11]. Hua Y, Zhang Y, Ceylan-Isik AF, Wold LE, Nunn JM, Ren J, Chronic Akt activation accentuates aging-induced cardiac hypertrophy and myocardial contractile dysfunction: role of autophagy, Basic research in cardiology, 106 (2011) 1173–1191. [PubMed: 21901288]

[12]. Turdi S, Fan X, Li J, Zhao J, Huff AF, Du M, Ren J, AMP-activated protein kinase deficiency exacerbates aging-induced myocardial contractile dysfunction, Aging Cell, 9 (2010) 592–606. [PubMed: 20477759]

[13]. Pillai VB, Sundaresan NR, Gupta MP, Regulation of Akt signaling by sirtuins: its implication in cardiac hypertrophy and aging, Circ Res, 114 (2014) 368–378. [PubMed: 24436432]

[14]. Ock S, Lee WS, Ahn J, Kim HM, Kang H, Kim HS, Jo D, Abel ED, Lee TJ, Kim J, Deletion of IGF-1 Receptors in Cardiomyocytes Attenuates Cardiac Aging in Male Mice, Endocrinology, 157 (2016) 336–345. [PubMed: 26469138]

[15]. Burkewitz K, Zhang Y, Mair WB, AMPK at the nexus of energetics and aging, Cell Metab, 20 (2014) 10–25. [PubMed: 24726383]

[16]. Wang S, Ge W, Harns C, Meng X, Zhang Y, Ren J, Ablation of toll-like receptor 4 attenuates aging-induced myocardial remodeling and contractile dysfunction through NCoRIHDAC1-mediated regulation of autophagy, J Mol Cell Cardiol, 119 (2018) 40–50. [PubMed: 29660306]

[17]. Bhide S, Trujillo AS, O'Connor MT, Young GH, Cryderman DE, Chandran S, Nikravesh M, Wallrath LL, Melkani GC, Increasing autophagy and blocking Nrf2 suppress laminopathy-induced age-dependent cardiac dysfunction and shortened lifespan, Aging cell, 17 (2018) e12747. [PubMed: 29575479]

[18]. Li Y, Ma Y, Song L, Yu L, Zhang L, Zhang Y, Xing Y, Yin Y, Ma H, SIRT3 deficiency exacerbates p53/Parkinmediated mitophagy inhibition and promotes mitochondrial dysfunction: Implication for aged hearts, International journal of molecular medicine, 41 (2018) 3517–3526. [PubMed: 29532856]

[19]. Zhang Y, Wang C, Zhou J, Sun A, Hueckstaedt LK, Ge J, Ren J, Complex inhibition of autophagy by mitochondrial aldehyde dehydrogenase shortens lifespan and exacerbates cardiac aging, Biochimica et biophysica acta, 1863 (2017) 1919–1932. [PubMed: 28347844]

[20]. Shirakabe A, Ikeda Y, Sciarretta S, Zablocki DK, Sadoshima J, Aging and Autophagy in the Heart, Circulation research, 118 (2016) 1563–1576. [PubMed: 27174950]

[21]. C ON, PI3-kinase/Akt/mTOR signaling: impaired on/off switches in aging, cognitive decline and Alzheimer's disease, Experimental gerontology, 48 (2013) 647–653. [PubMed: 23470275]

[22]. Yang S, Long LH, Li D, Zhang JK, Jin S, Wang F, Chen JG, beta-Guanidinopropionic acid extends the lifespan of Drosophila melanogaster via an AMP-activated protein kinasedependent increase in autophagy, Aging cell, 14 (2015) 1024–1033. [PubMed: 26120775]

[23]. Lotfi P, Tse DY, Di Ronza A, Seymour ML, Martano G, Cooper JD, Pereira FA, Passafaro M, Wu SM, Sardiello M, Trehalose reduces retinal degeneration, neuroinflammation and storage burden caused by a lysosomal hydrolase deficiency, Autophagy, (2018) 1–16.

[24]. Viollet B, Andreelli F, Jorgensen SB, Perrin C, Geloen A, Flamez D, Mu J, Lenzner C, Baud O, Bennoun M, Gomas E, Nicolas G, Wojtaszewski JF, Kahn A, Carling D, Schuit FC, Birnbaum MJ, Richter EA, Burcelin R, Vaulont S, The AMP-activated protein kinase alpha2 catalytic subunit controls whole-body insulin sensitivity, The Journal of clinical investigation, 111 (2003) 91–98. [PubMed: 12511592]

[25]. Cho H, Mu J, Kim JK, Thorvaldsen JL, Chu Q, Crenshaw EB 3rd, Kaestner KH, Bartolomei MS, Shulman GI, Birnbaum MJ, Insulin resistance and a diabetes mellitus-like syndrome in mice lacking the protein kinase Akt2 (PKB beta), Science, 292 (2001) 1728–1731. [PubMed: 11387480]

[26]. Boyle AJ, Shih H, Hwang J, Ye J, Lee B, Zhang Y, Kwon D, Jun K, Zheng D, Sievers R, Angeli F, Yeghiazarians Y, Lee R, Cardiomyopathy of aging in the mammalian heart is characterized by myocardial hypertrophy, fibrosis and a predisposition towards cardiomyocyte apoptosis and autophagy, Experimental gerontology, 46 (2011) 549–559. [PubMed: 21377520]

[27]. Pan B, Xu ZW, Xu Y, Liu LJ, Zhu J, Wang X, Nan C, Zhang Z, Shen W, Huang XP, Tian J, Diastolic dysfunction and cardiac troponin I decrease in aging hearts, Archives of biochemistry and biophysics, 603 (2016) 20–28. [PubMed: 27184165]

[28]. Ceylan-Isik AF, Dong M, Zhang Y, Dong F, Turdi S, Nair S, Yanagisawa M, Ren J, Cardiomyocyte-specific deletion of endothelin receptor A rescues aging-associated cardiac hypertrophy and contractile dysfunction: role of autophagy, Basic research in cardiology, 108 (2013) 335. [PubMed: 23381122]

[29]. Garofalo RS, Orena SJ, Rafidi K, Torchia AJ, Stock JL, Hildebrandt AL, Coskran T, Black SC, Brees DJ, Wicks JR, McNeish JD, Coleman KG, Severe diabetes, agedependent loss of adipose tissue, and mild growth deficiency in mice lacking Akt2/PKB beta, The Journal of clinical investigation, 112 (2003) 197–208. [PubMed: 12843127]

[30]. Shinmura K, Tamaki K, Sano M, Murata M, Yamakawa H, Ishida H, Fukuda K, Impact of long-term caloric restriction on cardiac senescence: caloric restriction ameliorates cardiac diastolic dysfunction associated with aging, J Mol Cell Cardiol, 50 (2011) 117–127. [PubMed: 20977912]

[31]. Chen X, Zhao X, Cai H, Sun H, Hu Y, Huang X, Kong W, Kong W, The role of sodium hydrosulfide in attenuating the aging process via PI3K/AKT and CaMKKbeta/AMPK pathways, Redox Biol, 12 (2017) 987–1003. [PubMed: 28499253]

[32]. Ronnebaum SM, Patterson C, The FoxO family in cardiac function and dysfunction, Annu Rev Physiol, 72 (2010) 81–94. [PubMed: 20148668]

[33]. Wang S, Zhu X, Xiong L, Ren J, Ablation of Akt2 prevents paraquat-induced myocardial mitochondrial injury and contractile dysfunction: Role of Nrf2, Toxicol Lett, 269 (2017) 1–14. [PubMed: 28115273]

[34]. Bjedov I, Toivonen JM, Kerr F, Slack C, Jacobson J, Foley A, Partridge L, Mechanisms of life span extension by rapamycin in the fruit fly Drosophila melanogaster, Cell Metab, 11 (2010) 35–46. [PubMed: 20074526]

[35]. Iida RH, Kanko S, Suga T, Morito M, Yamane A, Autophagic-lysosomal pathway functions in the masseter and tongue muscles in the klotho mouse, a mouse model for aging, Mol Cell Biochem, 348 (2011) 89–98. [PubMed: 21082218]

[36]. Cuervo AM, Bergamini E, Brunk UT, Droge W, Ffrench M, Terman A, Autophagy and aging: the importance of maintaining “clean” cells, Autophagy, 1 (2005) 131–140. [PubMed: 16874025]

[37]. Zhang C, Cuervo AM, Restoration of chaperone-mediated autophagy in aging liver improves cellular maintenance and hepatic function, Nat Med, 14 (2008) 959–965. [PubMed: 18690243]

[38]. Taneike M, Yamaguchi O, Nakai A, Hikoso S, Takeda T, Mizote I, Oka T, Tamai T, Oyabu J, Murakawa T, Nishida K, Shimizu T, Hori M, Komuro I, Shirasawa T, Mizushima N, Otsu K, Inhibition of autophagy in the heart induces age-related cardiomyopathy, Autophagy, 6 (2010) 600–606. [PubMed: 20431347]

[39]. Harrison DE, Strong R, Sharp ZD, Nelson JF, Astle CM, Flurkey K, Nadon NL, Wilkinson JE, Frenkel K, Carter CS, Pahor M, Javors MA, Fernandez E, Miller RA, Rapamycin fed late in life extends lifespan in genetically heterogeneous mice, Nature, 460 (2009) 392–395. [PubMed: 19587680]

[40]. Zhang Y, Sowers JR, Ren J, Targeting autophagy in obesity: from pathophysiology to management, Nat Rev Endocrinol, 14 (2018) 356–376. [PubMed: 29686432]

[41]. Saha S, Panigrahi DP, Patil S, Bhutia SK, Autophagy in health and disease: A comprehensive review, Biomed Pharmacother, 104 (2018) 485–495. [PubMed: 29800913]

[42]. Hansen M, Rubinsztein DC, Walker DW, Autophagy as a promoter of longevity: insights from model organisms, Nat Rev Mol Cell Biol, (2018).

Research highlights

- We examined the effect of Akt2-AMPK double ablation on cardiac anomalies in 12-month-old mice
- Akt2-AMPK double knockout unmasked age-induced cardiac contractile anomalies
- The effect of Akt2-AMPK double ablation was related to loss of autophagy and mitophagy

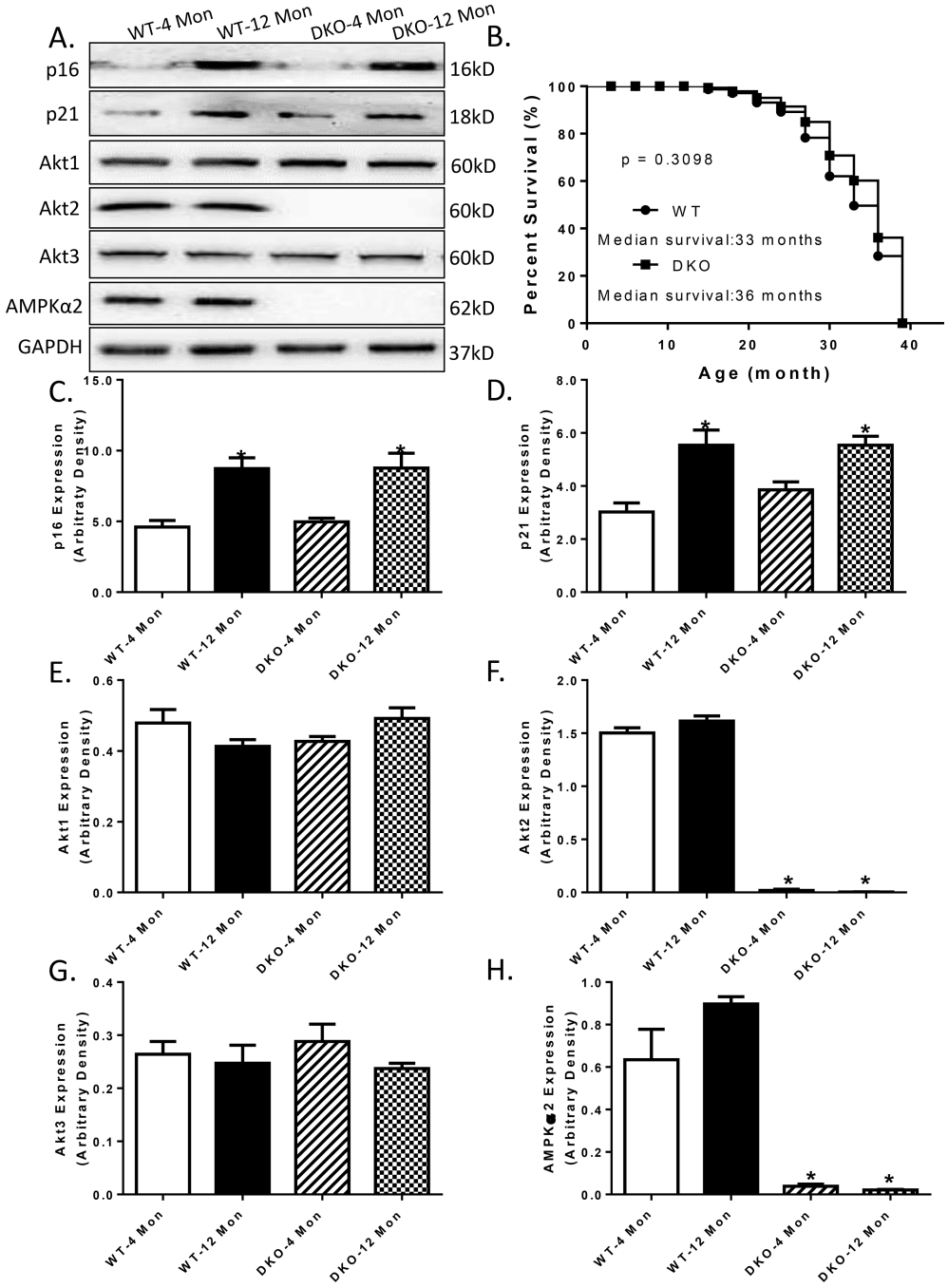

Fig.1:

Cumulative survival curve, aging markers, Akt isoforms and AMPKα2 expressions in WT and Akt2-AMPKα2 double knockout (DKO) mice. A: Representative gel blots depicting p16, p21, Akt1, Akt2, Akt3, AMPKα2 and GAPDH (loading control) levels using specific antibodies in 4- and 12 month-old mice; B: The Kaplan–Meier cumulative survival rate plotted against age in months in WT and DKO mice. The log-rank test was performed to compare the two curves (p = 0.3098). C: p16 expression; D: p21 expression; E: Akt1 expression; F: Akt2 expression; G: Akt3 expression; and H: AMPKα2 expression. Mean ±

SEM, n = 29–30 mice per group for panel B; n = 3 mice per group for panel C-H, *p < 0.05 *vs.* WT-4 month-old group.

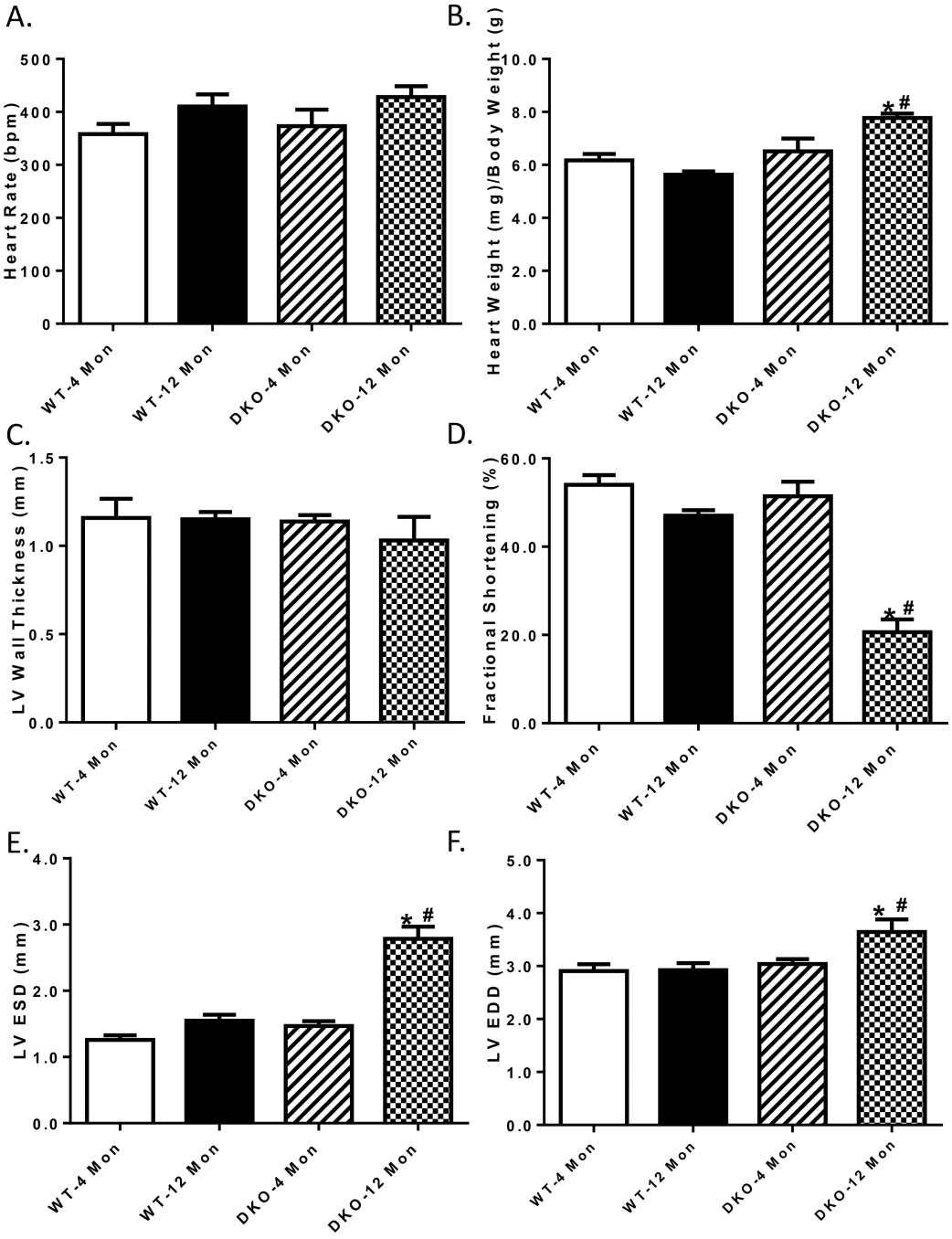

Fig.2:

Cardiac contractile function in 4- and 12 month-old WT and Akt2-AMPKα2 double knockout (DKO) mice. A: Heart rate; B: Normalized left ventricular (LV) mass; C: LV wall thickness; D: Fractional shortening; E: LV end systolic diameter (LVESD); and F: LV end diastolic diameter (LVEDD). Mean ± SEM, n = 5–8 mice per group. *p < 0.05 *vs.* WT-4 monthold group, # p < 0.05 *vs.* WT-12 month-old group.

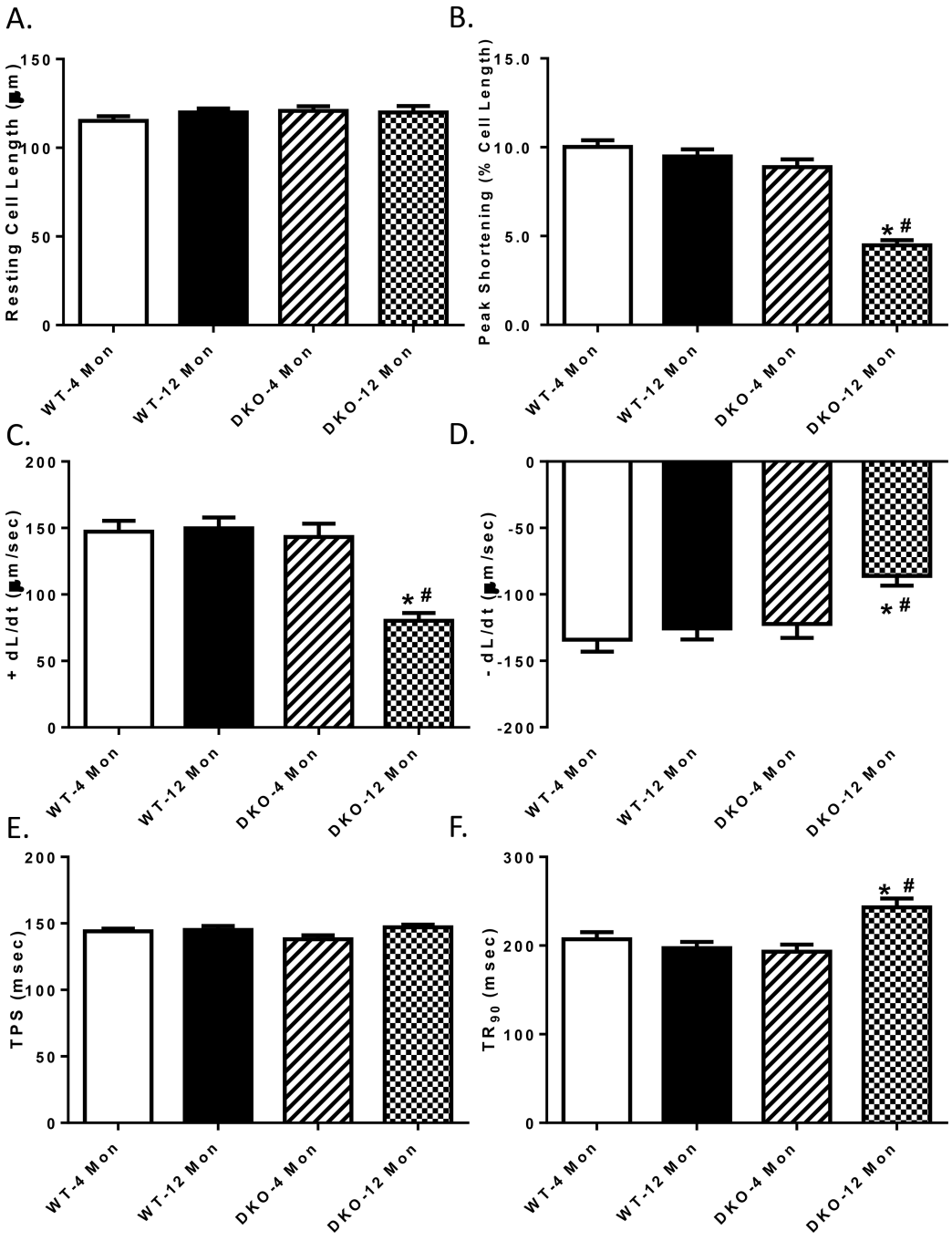

Fig. 3:

Contractile properties of cardiomyocytes from 4- and 12 month-old WT and Akt2-AMPKα2 double knockout (DKO) mice. A: Resting cell length; B: Peak shortening (normalized to cell length); C: Maximal velocity of shortening (+ dL/dt); D: Maximal velocity of relengthening (– dL/dt); E: Time-to–peak shortening (TPS); and F: Time-to-90% relengthening (TR_{90}); Mean ± SEM, n = 90 cells from 5 mice per group. *p < 0.05 *vs.* WT-4 month-old group, # p < 0.05 *vs.* WT-12 month-old group.

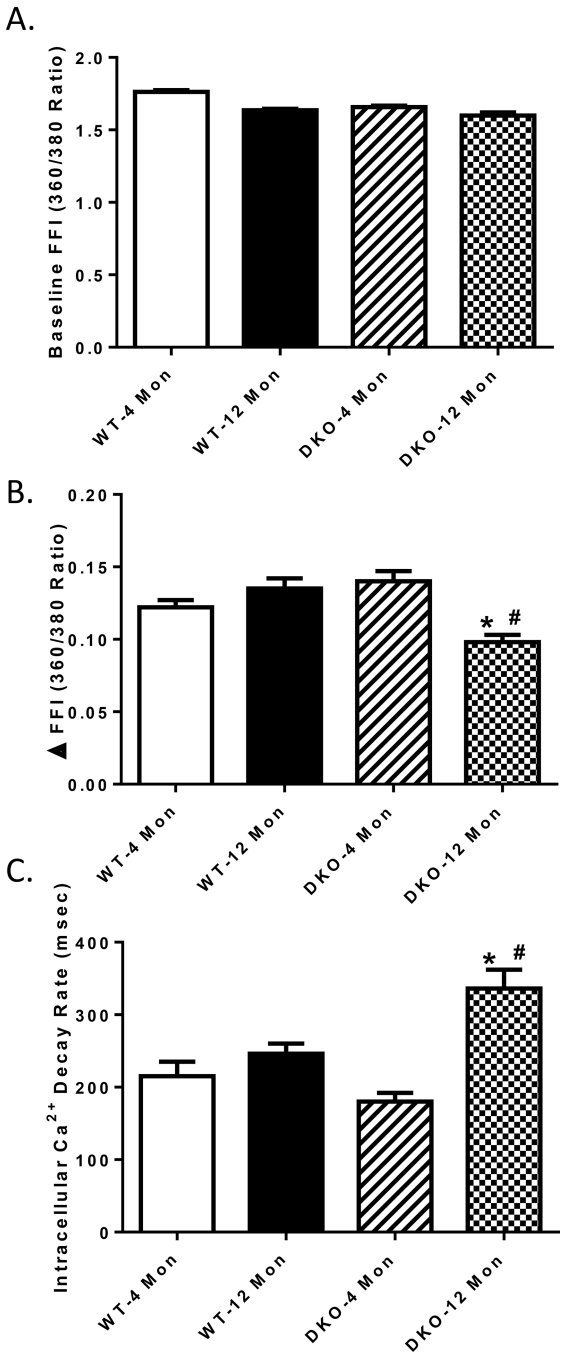

Fig. 4:

Intracellular Ca^{2+} homeostasis of cardiomyocytes from 4- and 12 month-old WT and Akt2-AMPKα2 double knockout (DKO) mice. A: Resting fura-2 fluorescence intensity (FFI); B: Electrically stimulated rise in FFI (ΔFFI) and C: Single exponential intracellular Ca^{2+} decay. Mean ± SEM, n = 60–65 cells from 5 mice per group. *$p < 0.05$ *vs.* WT-4 month-old group, # $p < 0.05$ *vs.* WT-12 month-old group.

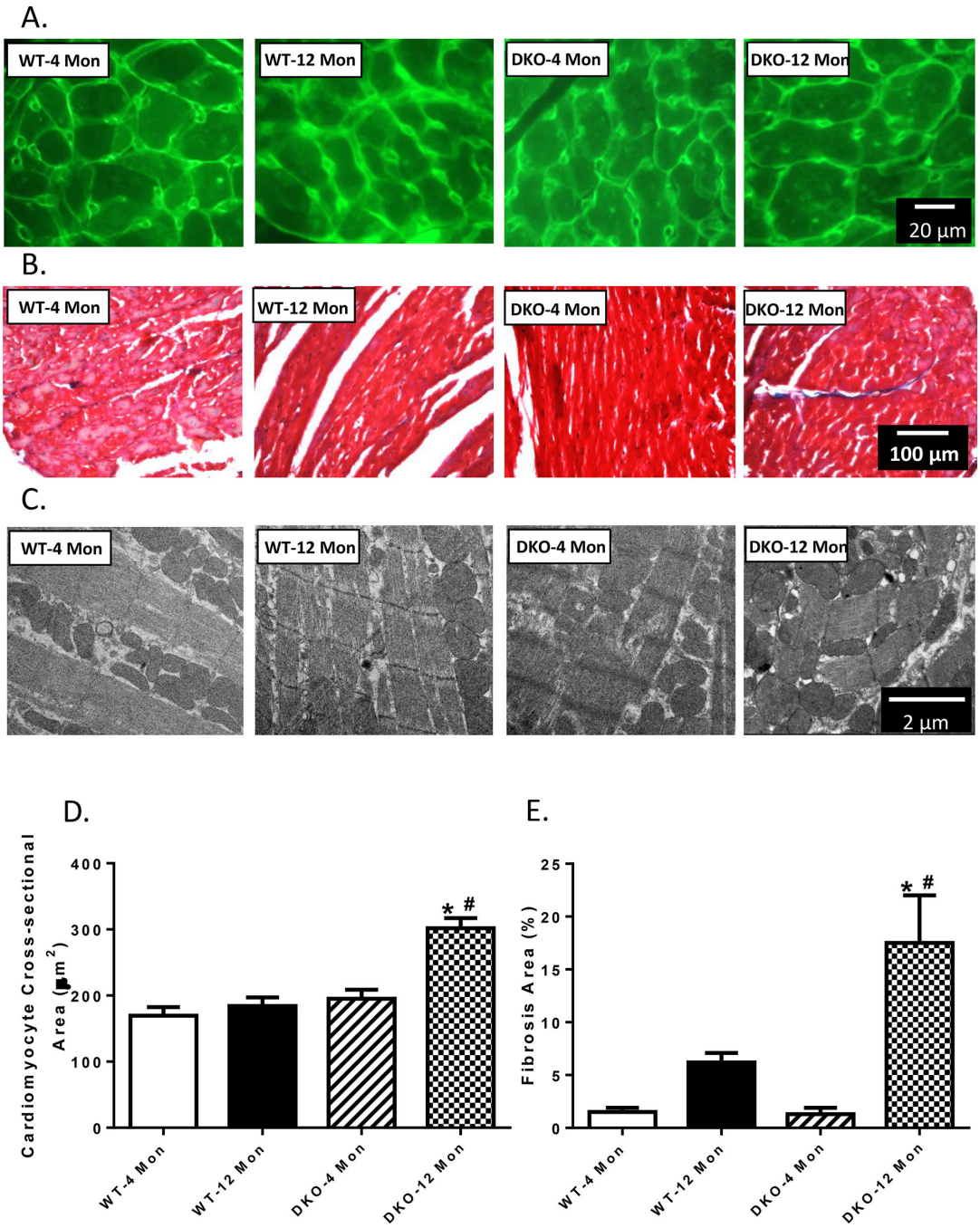

Fig. 5:

Myocardial morphology and ultrastructure in 4- and 12 month-old WT and Akt2-AMPKα2 double knockout (DKO) mice. A: Representative FITC-conjugated lectin staining depicting the transverse sections of left ventricular myocardium (×400); B: Representative Masson trichrome staining depicting fibrosis formation; C: Mitochondria and sarcomere ultrastructure using transmission electron microscopy. D: Quantitative analysis of cardiomyocyte cross-sectional area; and E: Quantitative analysis of fibrotic area (Masson's trichrome-stained area in light blue color normalized to the total myocardial area). Mean ±

SEM, n = 9–12 mice per group. *p < 0.05 *vs.* WT-4 month-old group, # p < 0.05 *vs.* WT-12 month-old group.

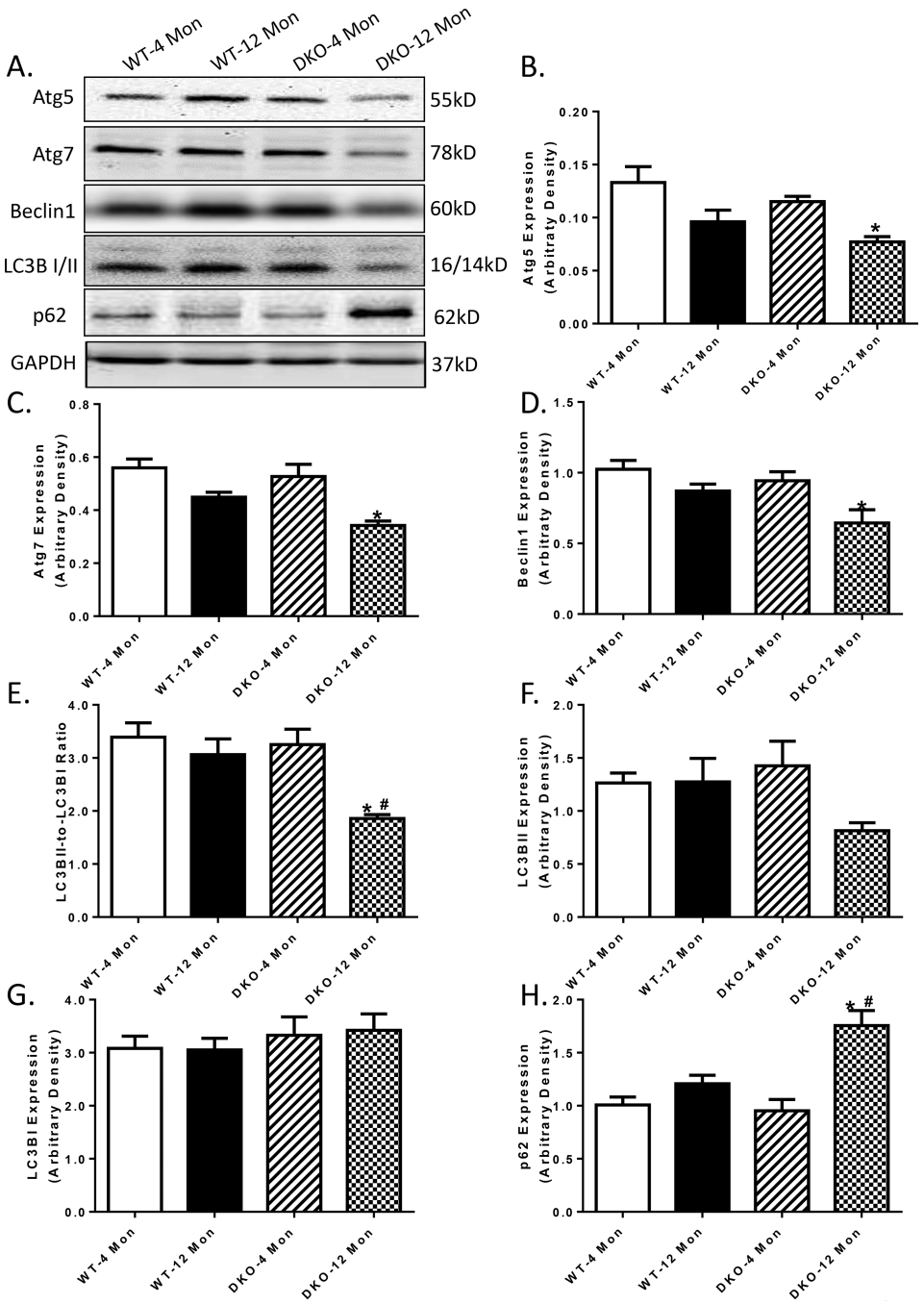

Fig. 6:

Autophagy marker expression in 4- and 12 month-old WT and Akt2-AMPKα2 double knockout (DKO) mice. A: Representative gel blots depicting levels of Atg5, Atg7, Beclin1, LC3B I/II, p62 and GAPDH (loading control) using specific antibodies; B: Atg5 expression; C: Atg7 expression; D: Beclin1 expression; E: LC3B II-to-I ratio; F: LC3B II expression; G: LC3B I expression; and H: p62 expression; Mean ± SEM, n = 9–15 mice per group. *p < 0.05 *vs.* WT-4 month-old group, # p < 0.05 *vs.* WT-12 month-old group.

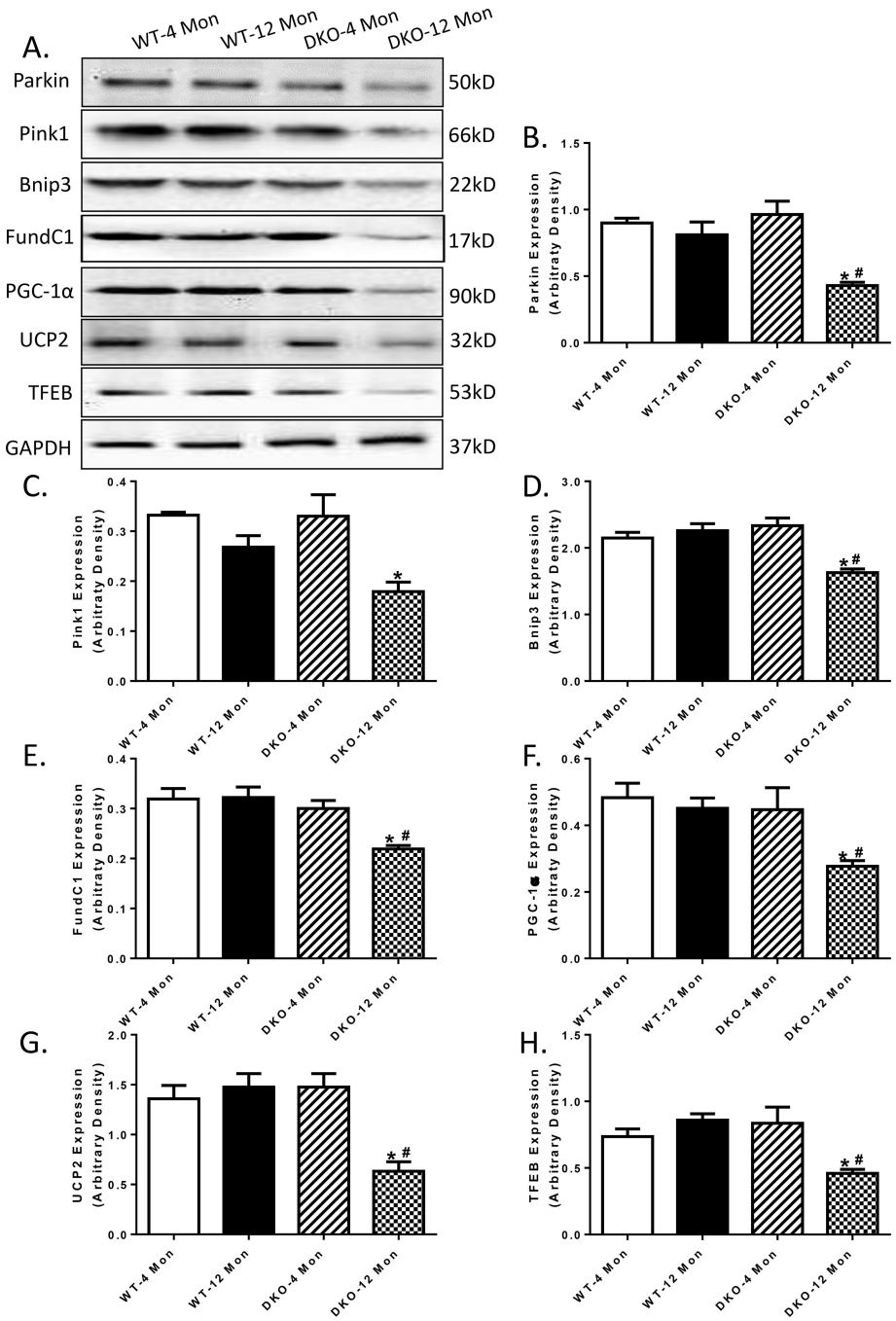

Fig. 7:

Mitophagy, mitochondrial markers and lysosomal biogenesis in 4- and 12 month-old WT and Akt2-AMPKα2 double knockout (DKO) mice. A: Representative gel blots depicting levels of Parkin, Pink1, Bnip3, FundC1, PGC-1α, UCP2, TFEB and GAPDH (loading control) using specific antibodies; B: Parkin expression; C: Pink1 expression; D: Bnip3 expression; E: FundC1 expression; F: PGC-1α expression; G: UCP2 expression; and F:

TFEB expression. Mean ± SEM, n = 6–11 mice per group. *p < 0.05 *vs.* WT-4 month-old group, # p < 0.05 *vs.* WT-12 month-old group.

Table 1:

General characteristics of in 4 month-old and 12 month-old WT mice and Akt2 and AMPKα2 knockout (DKO) mice.

Parameter	WT-4 Mon	WT-12 Mon	DKO-4 Mon	DKO-12 Mon
Body Weight (BW, g)	25.9 ± 0.8	29.4 ± 0.4	22.9 ± 1.5	27.4 ± 1.5
Tibial Length (mm)	18.2 ± 0.4	20.7 ± 0.4 *	17.0 ± 0.2	18.8 ± 0.5 *
Heart Weight (HW, mg)	154 ± 5	165 ± 3	141 ± 10	192 ± 6 *#
HW/BW (mg/g)	5.96 ± 0.21	5.63 ± 0.10	6.23 ± 0.39	7.12 ± 0.28 *#
Liver Weight (LW, g)	1.27 ± 0.03	1.49 ± 0.02 *	1.17 ± 0.06	1.31 ± 0.03 #
LW/BW (mg/g)	49.2 ± 1.7	50.7 ± 1.0	51.6 ± 1.5	52.4 ± 2.0
Kidney Weight (KW, g)	0.312 ± 0.009	0.379 ± 0.006 *	0.305 ± 0.005	0.369 ± 0.006 *
KW/BW (mg/g)	12.1 ± 0.4	12.9 ± 0.3	13.8 ± 0.7	13.8 ± 0.6
Spleen Weight (SW, g)	0.087 ± 0.005	0.162 ± 0.006 *	0.083 ± 0.004	0.162 ± 0.014 *
Glucose (mg/dl)	97.8 ± 5.1	97.1 ± 5.0	99.9 ± 5.1	103.0 ± 5.8
Insulin (ng/ml)	0.094 ± 0.010	0.244 ± 0.023 *	0.088 ± 0.010	0.272 ± 0.030 *
Triglyceride (mg/dl)	69.4 ± 4.5	80.3 ± 4.1 *	63.7 ± 6.3	88.1 ± 8.3 *

Mean ± SEM, n = 6–10 mice per group,

* $p < 0.05$ *vs.* WT-4 month group;

# $p < 0.05$ *vs.* WT-12 month group.